Coulomb explosions of dusty plasma confined in an ITO glass box

J. S. Rosenberg, Jorge Carmona-Reyes, Jimmy Schmoke, Lorin S. Matthews, and Truell W. Hyde

***Abstract*—Dusty plasma can be studied inside of a Gaseous Electronic Conference radio frequency reference cell. A glass box is placed in the reference cell and dust particles are dropped inside the box as a means of observing Coulomb explosions. To create these explosions the box is biased with a dc voltage to force the particles together. The bottom electrode of the reference cell was also changed at times to test the ability to create Coulomb explosions through changing the rf voltage. We observed that both changing the dc current on the box and the rf supply to the bottom electrode lead to particles falling, but did not see the expected Coulomb explosion. The equations and setup of the experiment must be reconsidered to include forces that were deemed miniscule and a setup that leads to three-dimensional tracking of the particles.**

***Index Terms*—Complex Plasma, Diagnostics, Image Analysis, Interaction Force, Particle Tracking.**

I. Introduction

Dusty plasma is often studied for its ability to allow us to macroscopically see interactions between particles that follow the same phenomenology as molecules that are detectable only with a sophisticated means of detection [1], [2]. Size is not the only aspect of dusty plasma that makes it a convenient alternative, but the interactions are also on a manageable time scale allowing us to see the processes in which we are interested.

We chose melamine resin (MF) particles with a diameter of 8.89 μm, which are very uniform in shape [3]. These dust particles are electrically neutral in nature, but once introduced into the plasma, which, in our case, is ionized argon gas, they gain a negative charge due to their interaction with the free plasma electrons [4]. Gravity is working simultaneously and so the particles are pulled down through the plasma to the sheath. The dust particles, now with a negative charge, are also repulsed by the electric field induced by negatively charged radio-frequency (rf) driven bottom electrode. This equilibrium of the gravity and electric field occurs in what is known as the ion rich plasma sheath. Our goal is to study the Coulomb explosion, which we are able to reproduce through the confinement of dusty plasma, by means of a glass box coated with iridium titanium oxide (ITO).

Manuscript received August 4, 2014. This work was supported by the National Science Foundation Grant 1262031.

J. Carmona-Reyes, J. Schmoke, L. S. Matthews, and T.W. Hyde are with the Center for Astrophysics, Space Physics, and Engineering Research, Baylor University, Waco, TX 76798 USA.

J. S. Rosenberg was with the Center for Astrophysics, Space Physics, and Engineering Research, Baylor University, Waco, TX 76798 USA, as a Research Experience for Undergraduates Student, and is currently an undergraduate of Colby College, Waterville, ME 04901 USA (email: jsrosenb@colby.edu).

II. Experiment

A. General Setup

In order to study dusty plasma, we have to make sure that it stays, well, dusty. We use a Gaseous Electronics Conference radio-frequency reference cell (GEC reference cell) [5]. The reference cell is equipped with dishes that are placed on the lower electrode. These dishes have different types of cutouts that help create a potential well so that our dusty plasma, well stays dusty, as can be seen in Fig 1 below.

Fig 1.This is a view of a dish with a 1 mm deep and 25.4 mm diameter cutout.

We can also drop the dust into the ITO box, which allows for even greater control of the dust particles by means of confinement, which is what we decided to use. We control the ITO box through a KEPCO external power supply, which is in contact with the box's ITO coating.

Dust particles inside the plasma act as microscopic probes. They react to all the forces involved in the system; however, in these experiments the only forces that were considered were those coming from the ITO box potential and the rf potential. All other forces are assumed to be of either one or two orders of magnitude smaller in comparison [6]. We were able to experiment with changes to both the voltage applied to the ITO box and the rf power supplied to the bottom electrode.

We directed our changes at confining the particles close together. We confined the particles by negatively biasing the ITO box, which induced inward radial forces. We proceeded to see how close the particles could get before their Coulomb interparticle forces far exceeded those forces inward from the box, that they repulse each other so much that they create a Coulomb explosion [4].

We used a GEC RF reference cell as described in previous work, though we will reiterate the vital information here and include a diagram from this previous work as can be seen in Fig 2 [7]. Our setup always included an ITO box and a cutout, where the cutout is the only aspect of our setup not in Fig 2 but is visible in Fig 3. The box has a height of 0.5 inches placed 2 mm above the bottom electrode so that they were not in direct contact with one another as can be seen in Fig 3.

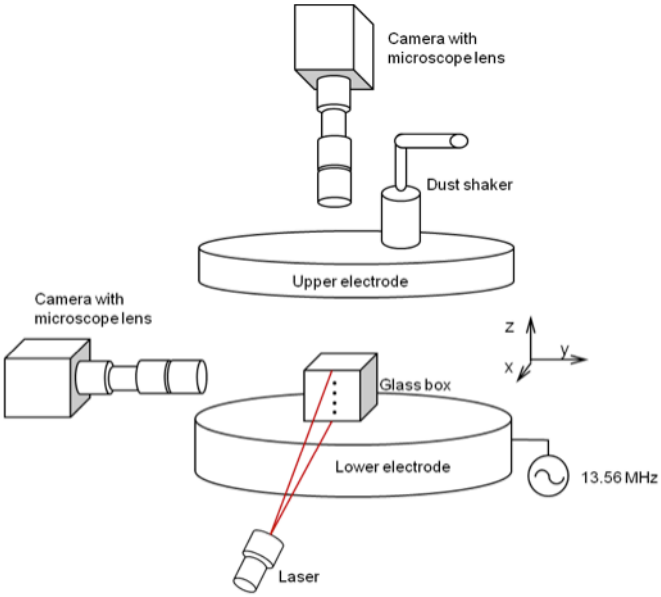

Fig 2. GEC reference cell from previous work [7]

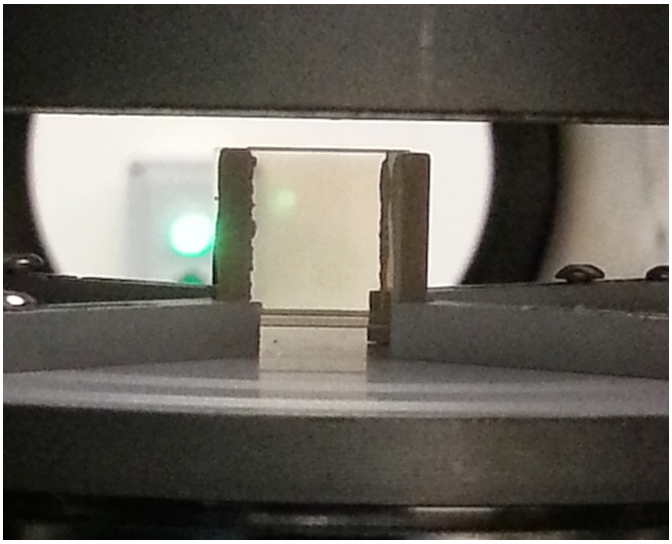

Fig 3. ITO box placed in the GEC reference cell on the bottom electrode.

As discussed earlier, the box is glass and coated with ITO and this allows us to attach all four sides of the box to a dc voltage supply and bias the box evenly. A signal generator and an amplifier drove the bottom electrode with a frequency of 13.56 MHz and a shunt network connected to the bottom electrode while the top electrode was grounded. We assumed the reference cell system was at room temperature while we varied other parameters, such as vacuum pressure and system power.

In order to observe the dust particles, we used a side or top StingRay illumination 100 mW Laser with a cylindrical lens and a camera with horizontal and vertical options as well. We found the best orientation was the side laser with the side camera. We used the laser solely for illuminating the dust particles and we assume it did not add kinetic energy to the system based off of work done by Liu et al [8]. The camera is a FASTCAM 1024 PCI with a CMOS sensor and a frame rate up to 1,000 frames per second (fps) at full resolution and reduced resolution up to 109,500 fps [9].

No two sets of data are the same; it behooves us to go through each setup along with the results.

B. Early Difficulties with the Experiment

Our first set of data, was used as a test to track particles, and was not an integral part the overall research of studying the confinement of the dust particles, which is why it is in the experiment section. What is important to note about this set of data is that we only introduced a few dust particles into the ITO box. At this stage, we knew that our other data sets would have a larger number of dust particles, which would make it much more difficult for us to assess the pitfalls of our analysis techniques. We took images of the dust particles at 500 fps and then used the plugin called MultiTracker for the software ImageJ/FIJI for analysis [10]. MultiTracker ended up being the plugin that we decided to use for all the data sets because it allowed us to produce the x and y coordinates of each particle for all the frames.

The first aspect that we realized we had to pay careful attention to for our analysis, was how many images we wanted. We first noticed that ImageJ had a very small amount of memory. We then proceeded to download FIJI instead, which is equipped with 5767MB against ImageJ's 3500MB. Even though 3500MB is a decent amount of memory, we did not want to encounter any issues after setting up our protocol.

The next detail we had to consider was how to extract the dust particles and differentiate them from their surroundings. We could not use MultiTracker without a background image that allows us to find a threshold difference between the background and what we are tracking.

To use the MultiTracker we first had to import all of the images of each experiment as an image sequence and then open the background image separately. After those two steps, we proceeded to use the image calculator to subtract the background image from the stack. The penultimate step is the only error-riddled part of the analysis. We had to use the threshold tool, which turns the particles, or any color difference from the background, into red. The problem with the threshold tool is that it is dependent on the background, which only affects some data sets and will be discussed as needed and can be seen in the following images. Fig 4, shows our dark background, while Figs 5(a), 5(b), 6(a), and 6(b), show how we have to be very careful which our threshold.

Fig 4: Background example, which is much darker than Fig 5.

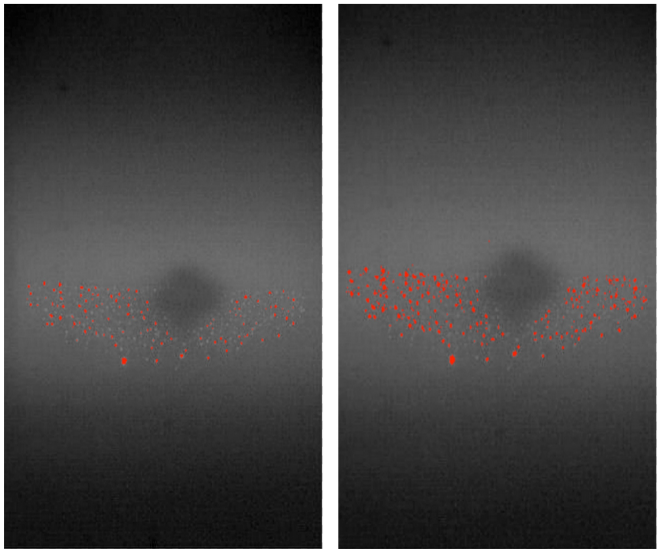

Fig 5. The left image 5(a) shows the threshold we used, while the right image 5(b) shows the threshold that does not work for later images.

The final step of the analysis is to (finally) run the MultiTracker, which yields coordinates of each of the particles that the threshold tool allowed us to recover. We were then able to save the coordinates as both a text file and an excel file.

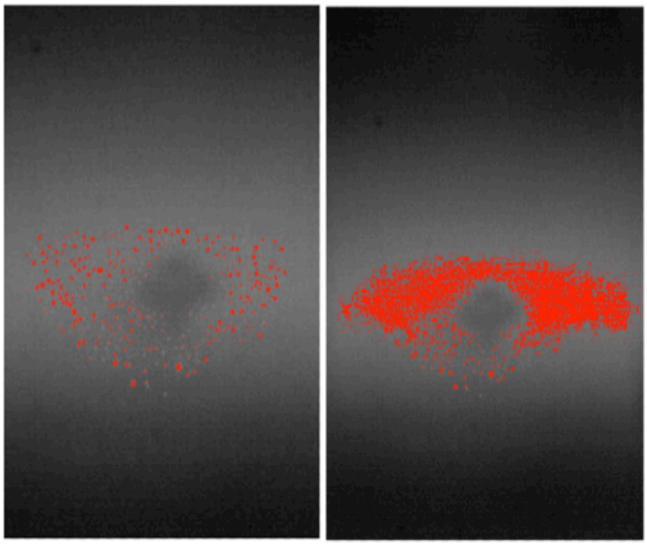

Fig 6. The left image 6(a) shows the threshold we used, while the right image 6(b) shows the threshold that does not work for later images.

An important detail about the MultiTracker is that if the camera's view of the particle is obstructed by another particle in one image, then MultiTracker will not be able to find the particle if it becomes visible again, even if it is only one frame later. An example of hidden particles can be seen in the Figs 7(a) and 7(b).

FIJI also has a calibration tool, which enabled us to utilize an image we took of a ruler inside the ITO box. We fed this image into FIJI and then could calculate the height from the bottom electrode to the top of the frame in both pixels and microns, and this image can be seen in Fig 8.

Knowing the height of the image from the bottom electrode is necessary for us to be able to utilize our MultiTracker data because the origin of the image is at the top left corner. We did not change the x coordinates in any way, but we noted that the MultiTracker assumes the left side of the image is the zero x coordinate.

We will discuss the effects of these aspects of MultiTracker as they pertain to data at hand.

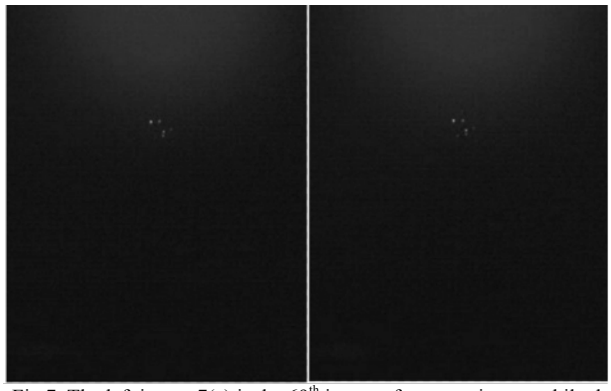

Fig 7. The left image 7(a) is the 69th image of an experiment, while the right image 7(b) is the 70th image of the same experiment where some particles are not visible that can be seen in Fig 7(a).

III. Data

A. Data Set One

In our first set of data, or Set 1, we were only able to track 78 MF dust particles inside the ITO box. The first thing we did, before we dropped the dust, was taking a picture of what would be our background. We then set the pressure at 330 mTorr, the plasma power to 4.75 W, the gas flow rate at 20.2 SCCMs, and then recorded the system natural bias (-184 V) which is obtained by passing the system rf voltage through a low pass filter with a cutoff frequency of 1kHz. We set the camera to 2000 fps because we were not sure what the best frame rate would be in order for us to have enough images that the particles are not blurry, but not too many that FIJI would run out of memory. We set the camera to take the images while we changed dc voltage on the ITO box from 0 V to -15 V. We started at 0 V because we wanted to begin the

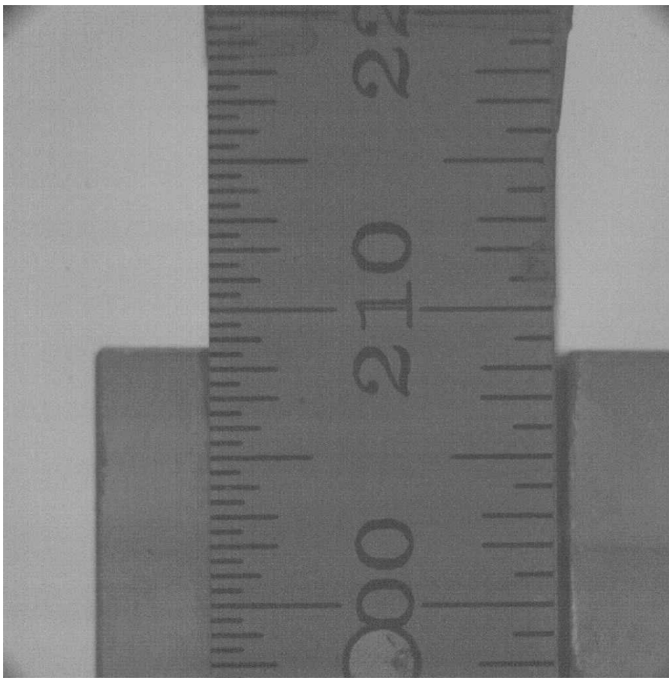

Fig 8. The size of the image is known to be 1024 x 1024 pixels in this calibration image.

experiment with no bias on the box, and then observe how a sudden inward force would effect the particles confinement. We chose to stop biasing the box at -15 V because of limitations that would cause the plasma to be unstable at -30 V and we chose to take the half waypoint to this physical limitation.

In the end, we had 2985 images, but we ended up only using images starting at frame number 2637 since the images up until that point were of no interest to us because the images showed no change in the dust cloud. There was no movement of the particles in the downward direction, which would be indicative of a Coulomb explosion. Therefore, we began our analysis at image 2637 and then we stop analyzing at image 2859, where image 2859 is indicated by red boxes in Figs 10(a) and 10(b) (red means stop!).

We made the voltage more negative on the ITO box, but it was a continuous change and so the voltage went through all the numbers in between 0 V and -15 V, and we cannot know exactly at what voltage the box was biased when the particles fell. What we can do though is look at features on the graphs and compare them to their corresponding images. When we look through the images in sequence, we easily observed that the particles start falling at image number 2759, which is shown in Fig 9(a).

Our frame rate was 2000 fps, so Figs 9(a) and 9(b) are 0.016 seconds apart from each other. It is easily observed from the graph of the average interparticle distance over time in Fig. 10(a) that there is no strong minimum, and in fact there is another, lower minimum after the particles have begun to fall. We expected the graph to show a drastic increase after reaching a minimum but the graph does not show this change.

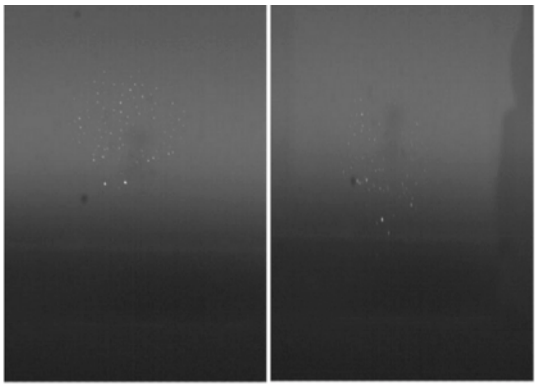

Fig 9. The left image 9(a) is Set 1, Image 2759 represented by the green data points in Figs 10(a) and 10(b). The right image 9(b) is Set 1, Image 2791 represented by the purple data points in Figs 10(a) and 10(b).

The features we expected to see on the graph would be indicative of the forces caused by the surface potential of the box, becoming greater than the interparticle interaction force at one point in time. Then, since the particles are negatively charged, they will first be strongly repelled by the box's force, and then the particles will become so close that the interparticle Coulomb repulsion will take over and produce the explosion. There should be some visible minimum of interparticle spacing, a critical point, where this switch of forces occurs [2].

Instead, we see the particles start to fall at frame 2759, which correlates to the green square on the graphs.

Granted, the images, Figs 9(a) and 9(b), to the naked eye give the unexpected appearance that the particles do just fall, and do not repel each other strongly.

The maximum peak in Fig. 10(a) is reached at about 2791, baring later images where only a few particles remain, yet there is no reason that this purple peak in Fig 10(a) should occur at frame 2791. We also tried to see how this graph in Fig 10(a) correlated with the graph of electrostatic force in Fig 10(b), and the colors on the two graphs correlate to the same time and frame.

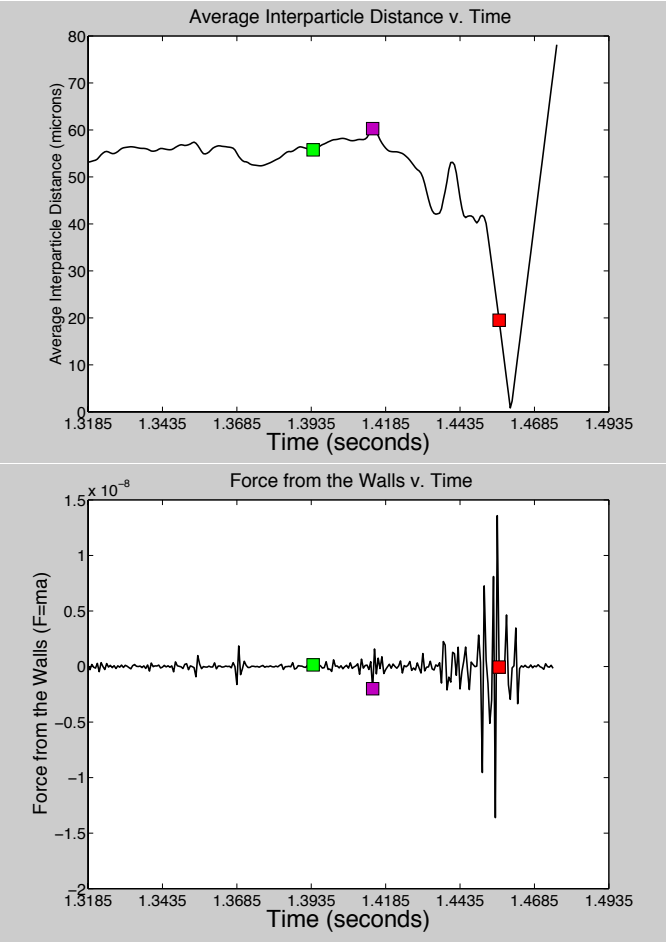

Fig 10. The top Fig 10(a) is Set 1 data graph of interparticle distance, while the bottom Fig 10(b) is the same data, Set 1, but a graph of the electrostatic force due to the walls of the box.

B. Data Set Two

If the plasma intensity in grey scale image changes we had to take note of what we could track and what could be lost. As can be seen by the clear loss of tracked particles in the following images in Figs 11(a) and 11(b), and their corresponding results images in Figs 11(c) and 11(d).

In this set of data, Set 2, we found that it was a little bit trickier to use the MultiTracker plugin because of the nature of how changing the rf voltage effects the image contrast, which lead us to only being able to fully track 117 particles, as shown in Figs 5, 6, and 11. We set the pressure for this experiment at 400 mTorr and then set the dc voltage on the box at -30 V and did not change it for the rest of the experiment. We also recorded the bias of the bottom electrode at -227 V and a flow rate of 20.6 SCCMs.

We proceeded to change the rf power from 31.25 W to a lower number that we cannot know because we lowered the power until (and a bit after) the particles fell. All we know is that the final plasma power was 13.6 W. The change in the plasma power can be easily observed in the change of the images' background color. The issue though, is that we see the color immediately coincide with the particles falling, but we cannot say what value the rf power was exactly when the change occurred.

When we look at the image sequence, we can see that image number 1202 (not shown here) is when the particles begin to fall, and by image 1214 we see substantially more particles dropping, as shown in Fig. 12.

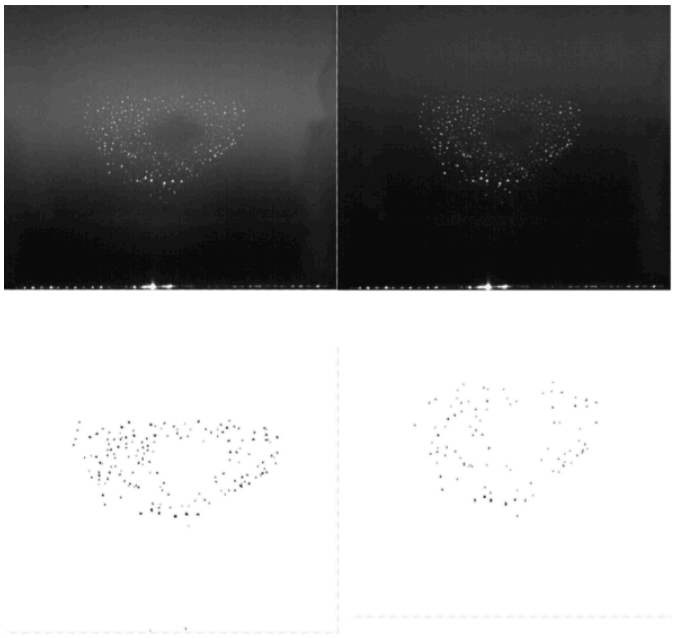

Fig 11. The top left Fig 11(a): Set 2, Image 1201. Top right Fig 11(b): Set 2, Image 1202. Bottom left Fig 11(c): Set 2, results Image 1201. Bottom right Fig 11(d): Set 2, results Image 1202.

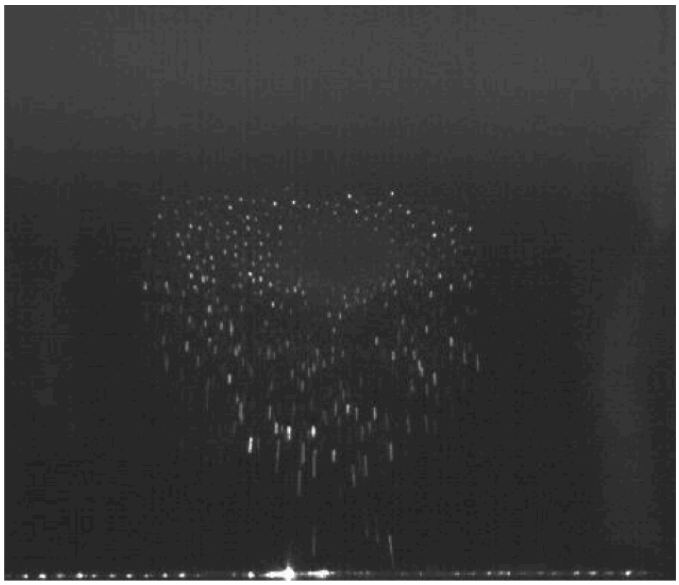

Fig 12. Set 2, Image 1214.

Our frame rate is 1500 fps with a total of 0.847 seconds of images, and so there is only a time difference of 0.0087 seconds between these images. This is an extremely obvious and drastic change in the particles absolute position. It has been researched that suddenly shutting the rf off suddenly leads to a very clear and strong repulsion [4]. In their experiment, they also used MF particles, though with a diameter of 4.8 μm. Their setup called for 5000 particles confined in a disk shape of diameter 2-3 mm, which is the same size as ours, though we have a box. They used three

different pressures, 30 Pa, 55 Pa, and 100 Pa. For the 30 Pa they noticed a large expansion in the x coordinate spread of the particles during the Coulomb explosion and smaller changes with each increasing pressure. Their setup was very similar, and so we expected to get similar results.

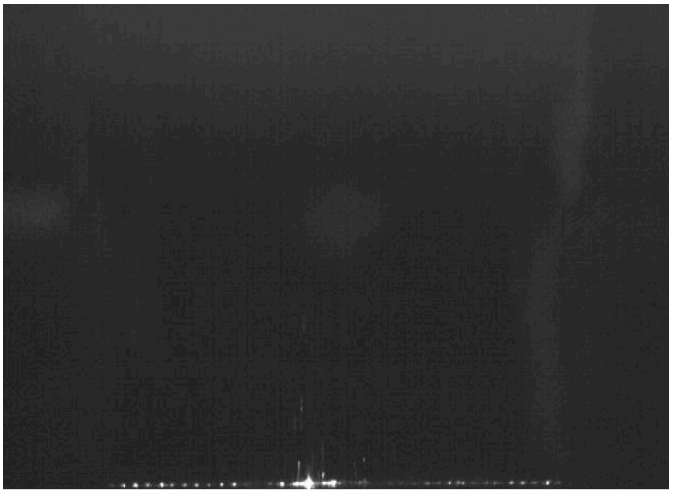

Fig 13. Set 2, Image 1259.

In Set 1, we expected to see drastic changes in our graphs of both the average interparticle space against time and the electrostatic force, also with respect to time. While we expected to see these results, we were a bit more surprised with this set, or Set 2, because of the experiments that showed drastic changes in the interparticle space, with smaller changes to the electrostatic force [4].

We already said that by sight, we would think that the graph should have some obvious change, since we can see these in the images. Frame 1259**,** or second 0.839, is where we have to stop trusting the graph due to the high error since only a few particles remain as can be seen in Fig 13.

We are therefore left with only a small segment of the graph in Fig 14(a) to analyze.

This graph in Fig 14(a) of the average interparticle distances is quite interesting.

The first green square in Fig 14(a) indicates where we started analyzing since it is the start of change in the particles' positions.

The purple square is interesting, because represents image 1201 (Fig 11(a)), which is the last image prior to the change in the plasma background, and the falling of the particles. Therefore, we would expect to see the purple square to be at a minimum; and the strangest part is that the space between the particles drastically decreases after the particles have started falling. The final red square, (still represents stop) shows the quick decent of the interparticle distance, and signifies the last points we can use. (The green squares mean go!)

A quick comparison with the graph showing the force in Fig 14(b), also gives inconclusive results.

Once again, the green box is the start of the change in the particles absolute position with the purple box as the sudden change in the plasma background. The electrostatic force appears to be strongest during the end of the experiment and not before the particles fall, which is unexpected.

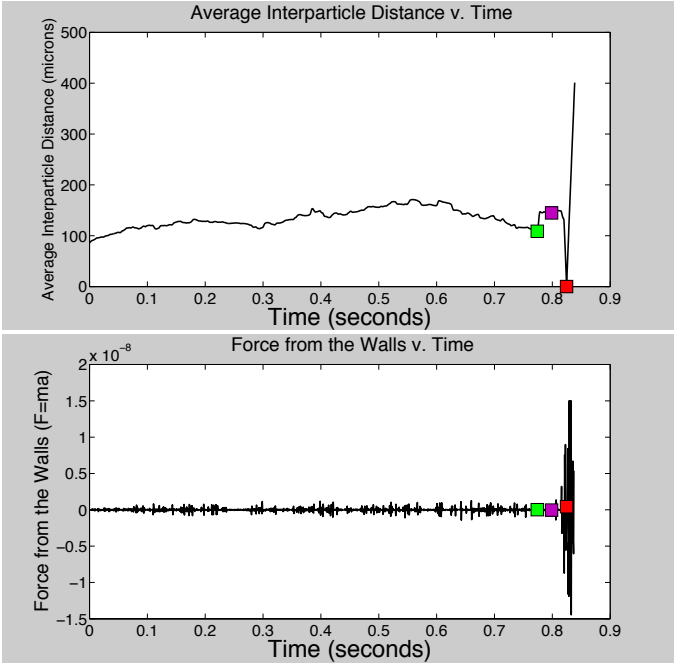

Fig 14. The top Fig 14(a) is Set 2 data graph of interparticle distance, while the bottom Fig 14(b) is the same data, Set 2, but a graph of the electrostatic force due to the walls of the box.

IV. Analysis

For all of the experiments we were able to create a MatLab code that took the positions generated by MultiTracker. The MultiTracker steps are extensive and so as not to lose sight of the big picture we will discuss this in a bit. The MatLab code we wrote calculated the particles' positions, velocity, and acceleration, with respect to both the x and y directions. We also calculated the average interparticle space for each frame as well as the average x position and y position.

We were able to calculate the average x and y positions without issues, as well as the velocity and acceleration. Since we already knew the frame rate and the number of images, we had time and each particles position; we used the change in position for our velocity equation and used those results for the acceleration.

Once we had finished the cut and dry equations, such as velocity and acceleration, we had to calculate the forces. We had to make some assumptions based off of the theory of Coulomb interactions and our experiment.

The forces acting on the dust particles inside the box are the same as when we do not use the box. Eq. (1) includes forces between the particles themselves and the dust cloud as a whole with the bottom electrode.

$$F_{total} = F_{coulomb} + F_{yukawa} + F_{ion\,drag} + F_{neutral\,drag} + F_{gravity} + F_{electric} \quad (1)$$

Even though we know which forces are in play, that does not mean that we can quantify them easily. In order to understand why, we can look at each force one at a time. The first force is the Coulomb force, as can be seen in Eq. (2).

$$F_{coulomb} = \frac{1}{4\pi\varepsilon_\circ}\frac{q_1 q_2}{r^2} \quad (2)$$

The Coulomb force is quite clearly of importance to our experiment. When we look at Eq. (2) though, we have variables representing the charges, the values of which has been reported in many references as somewhere between 10,000 to 100,000 electron charges [11]. If we knew the values of the charges on the dust particles, then we would have a very good understanding of at what distance the Coulomb explosion occurs.

The next force is the Yukawa force, which quite literally goes hand in hand with the Coulomb force and is represented with Eq. (3).

$$F_{yukawa} = \frac{1}{4\pi\varepsilon_\circ}\frac{q_1 q_2}{r^2}\, e^{\frac{r}{-\lambda_D}} \quad (3)$$

The Yukawa force is important in the same way that the Coulomb force is, because they are the same except for an extra term in the Yukawa force formula. This extra term is what allows us to also call the Yukawa force the screened Coulomb force [12]. The term includes values that we do not know. This includes the distance between the particles, and the Debye length, though the Debye length has been estimated outside of a glass box as between 52 μm and 405 μm [13]. The Debye length is denoted by $\lambda_D$and is the distance at which the particles will keep from each other in order to shield themselves from each other's electrostatic force. This distance allows for the particles to stay at a distance that means the Yukawa force is significantly greater than the Coulomb force.

Now, in theory, when we increased the dc voltage we decreased our distances between the particles, the r term becomes small enough that the extra term in the Yukawa force equation that is not present in the Coulomb force equation, becomes practically one.

As $e^{\frac{r}{-\lambda_D}} \to 1$ in Eq. (3), then the Yukawa force becomes the same equation as the Coulomb force, which means that the interactions between the particles are no longer shielded from each other, and they feel the complete brunt of the Coulomb forces.

Before we continue to discuss the other forces represented in the total force equation, we can see that if the total force only included the Coulomb and the Yukawa forces, it would look like Eq. (4)

$$F_{total} = F_{coulomb} + F_{yukawa} = \frac{1}{4\pi\varepsilon_\circ}\frac{q_1 q_2}{r^2} + \frac{1}{4\pi\varepsilon_\circ}\frac{q_1 q_2}{r^2}\, e^{\frac{r}{-\lambda_D}} \quad (4)$$

It is quite obvious that there should exist a point, some r, where the Coulomb force is significantly larger than the Yukawa, where prior to that point the exact opposite is true.

The next force we considered were the drag forces, which include those due to the neutrals, and the ions. These drag forces have been shown to be of at least one order of magnitude smaller, and its effect inside the ITO box is not understood, so we chose to leave them out of our calculations [6].

The final two forces are those due to the bottom electrode and, we cannot forget, gravity. There is a force that we could have added that would be due to added kinetic energy and reflected by the Brownian motion of the particles, but we ignore this force because we are assuming that the temperature is constant as we stated earlier [14].

The Yukawa and Coulomb forces both act isotropically. When the particles are at a distance longer than the screening length (Debye length), they are in equilibrium with the forces that are due to the walls of the ITO box, and do not feel the Coulomb force, which are electrostatic. When the interactions between the particles are Yukawa, then we know that the electrostatic force due to the walls is in balance with respect to the surface potential of the glass box's walls. However, there comes a time that as the potential on the glass walls increases that the particles interaction will mainly be dominated by the Coulomb force, which is why when they are to close to each other they repel each other and explode. We also assume that at the time of the particles dropping that the x component of the Coulomb force the sole cause of the inward force. Thus, we are left with Eq. (5).

$$F_{total} = F_{coulomb} = \frac{1}{4\pi\varepsilon_\circ}\frac{q_1 q_2}{r^2} = ma \quad (5)$$

We discussed above how the acceleration in both the x and y directions of the particles are calculated directly from the data and so no assumptions are made. That being said, we also have very accurate calculation for the mass of the dust particles. The company gives the density of the particles, and we know that we chose to use MF particles with a diameter of $8.89\ \mu m$ and the given density is $1.51\ g/cm^3$ [3]. The company also claims that the particles are very symmetrical spheres allowing us to calculate the mass using the equation for the volume of a sphere, Eq. (6).

$$V = \frac{4}{3}\pi r^3 \quad (6)$$

The forces in the y-direction keep the particles from falling, so we know that gravity and the electrostatic forces are equal during those times [12]. For analyzing the data, we did not make this assumption since the particles are not always in equilibrium. Instead, we calculate the downward force directly by using the acceleration in the y-direction, which as we already discussed as being intrinsic to the data and therefore returns a very small error. We calculated the mass to be $5.55 * 10^{-12}\ Kg$, and while the website does not state the margin for error, as we noted above the particles are uniformly spherical.

We have the ability now to graph the force of the walls on the particles, which we are using as equal to the interparticle forces, Coulomb forces, equated to ma_x, against both time and the number of frames. We also chose to graph the average interparticle distance against time and the number of frames, and we were able to match data points with our images allowing us to visually choose images that we believe should correlate to some change in the graphs.

We also graphed the average interparticle space against the number of frames and time to further examine another correlations we believe to exist. Once again, we hypothesized a threshold should be visible in the graph indicating a minimum point where the particles are as close together as possible and then the graph should rapidly increase indicating

the repulsion of the particles from one another and an explosion.

V. Conclusion And Future Work

The first set of graphs, we believe would show us a correlation between the particles falling and the force of the walls, which we equated to the interparticle forces. We believe that once the force reaches a threshold point, we should be able to see a drastic change in the force, possibly a sudden drop, and a falling of the particles. The particles should get so close together that they reach this minimum interparticle distance and then drop due to a sudden outward repulsion. We know that Coulomb explosions occur, many others have research Coulomb explosions; and it we know that a Coulomb explosion either happens or it does not; it cannot partially occur [4].

We also graphed the average interparticle space against the number of frames and time to further examine another correlation we believe to exist. Once again, we expected a threshold to be visible in the graph indicating a minimum point where the particles are as close together as possible and then the graph should rapidly increase indicating the repulsion of the particles from one another and an explosion. We did not see evidence of our hypothesis, and there can be many reasons for this. It is possible that we should not have expected a Coulomb explosion since we did not vary our experiment in the same way that Coulomb explosions were seen in earlier work [4]. As discussed, the earlier work turns the rf off very quickly, and it seems likely that they are changing multiple plasma variables and not just the interparticle distances. Another reason could be that we need to be able to track all the particles regardless of the change in the background. In order to have no issue with the background is to have two background images: one for each contrast change. There is another issue with having two backgrounds, and that is that MultiTracker cannot save which particle is which from run to run, so a better method would have to be found.

Another issue that needs further research is figuring out a way so that no particles are hidden, because we know that they will then not be tracked again. Of course losing sight of particles can also have its positives, like losing a possible non-particle that appears to be a particle, like some noise in the image. Though there are positives, we would also like to be able to find the z-component of each particle's position, which can also go hand in hand with not losing particles. If we use stereoscopy, as has been used for plasma research before, we will solve the issue of both the z-component and losing the particles, though even this research needs work [15], [16]. We also have to run more experiments, and possibly try and recreate previous experiments done by others to see if we at least get similar results of Coulomb explosions when we shut our rf off completely [4]. If we do not, we have to rethink the forces pertaining to the box. We already do not know what the potential of the box is, but we have our ideas, though if we would have to question our hypothesis.

The next steps should be done with extreme organization to explore the possibilities for our unexpected results. We already stated that we should shut the rf off completely to compare our results to others', but we must also not forget that there is a possibility that our analysis in MatLab may be flawed. Maybe, we cannot equate the electrostatic force to the mass multiplied by the acceleration; other forces may be more important than we thought when using the ITO box and that these assumptions left our MatLab code incapable of returning accurate analysis.

Though we did not see what we expected on the graphs of interparticle distance and the electrostatic force; the images were just as surprising. The particles appear to just fall, which we did not expect, but we believed that it was possible that the graphs would show the details that cannot be perceived with the human eye. Well, we did not get any of the expected results: no apparent minimum interparticle distance, no Coulomb explosion, and no obvious correlation between the average interparticle space and the electrostatic force. The lack of connections is just as interesting as if we had seen more links. Further research is needed to study the ITO box, and to find the particles' positions in all three dimensions.

Acknowledgment

Jessica S. Rosenberg would like to thank Mike Cook and Jimmy Schmoke for their help with the laboratory setup. She would also like to extend her deepest gratitude to Jorge Carmona-Reyes, Lorin S. Matthews, and Truell W. Hyde for all their guidance and support. Finally, none of this could be possible without the opportunity and funding from the CASPER Program and the National Science Foundation, and the wonderful support from my fellow REUs and RETs.

References

[1] Y. Ivanov and A. Melzer, "Modes of three-dimensional dust crystals in dusty plasmas," *Phys. Rev. E*, vol. 79, no. 3, p. 036402, 2009.

[2] A. Piel and J. A. Goree, "Collisional and collisionless expansion of Yukawa balls," *Phys. Rev. E*, vol. 88, no. 6, p. 063103, 2013.

[3] "Microparticles." [Online]. Available: http://microparticles.de/properties.html.

[4] T. Antonova, C.-R. Du, A. V. Ivlev, B. M. Annaratone, L.-J. Hou, R. Kompaneets, H. M. Thomas, and G. E. Morfill, "Microparticles deep in the plasma sheath: Coulomb 'explosion,'" *Phys. Plasmas 1994-Present*, vol. 19, no. 9, p. 093709, 2012.

[5] P. J. H. Jr, K. E. Greenberg, P. A. Miller, J. B. Gerardo, J. R. Torczynski, M. E. Riley, G. A. Hebner, J. R. Roberts, J. K. Olthoff, J. R. Whetstone, R. J. V. Brunt, M. A. Sobolewski, H. M. Anderson, M. P. Splichal, J. L. Mock, P. Bletzinger, A. Garscadden, R. A. Gottscho, G. Selwyn, M. Dalvie, J. E. Heidenreich, J. W. Butterbaugh, M. L. Brake, M. L. Passow, J. Pender, A. Lujan, M. E. Elta, D. B. Graves, H. H. Sawin, M. J. Kushner, J. T. Verdeyen, R. Horwath, and T. R. Turner, "The Gaseous Electronics Conference radio-frequency reference cell: A defined parallel-plate radio-frequency system for experimental and theoretical studies of plasma-processing discharges," *Rev. Sci. Instrum.*, vol. 65, no. 1, pp. 140–154, Jan. 1994.

[6] G. V. Paeva, *Sheath phenomena in dusty plasmas*. Technische Universiteit Eindhoven, 2005.

[7] J. Kong, K. Qiao, J. Carmona-Reyes, A. Douglass, Z. Zhang, L. S. Matthews, and T. W. Hyde, "Vertical interaction between dust particles confined in a glass box in a complex plasma," *Plasma Sci. IEEE Trans. On*, vol. 41, no. 4, pp. 794–798, 2013.

[8] B. Liu, J. Goree, V. Nosenko, and L. Boufendi, "Radiation pressure and gas drag forces on a melamine-formaldehyde microsphere in a dusty plasma," *Phys. Plasmas 1994-Present*, vol. 10, no. 1, pp. 9–20, 2003.

[9] "Photron." [Online]. Available: http://www.photron.com/?cmd=products&type=legacy.

[10] "MultiTracker." [Online]. Available: http://rsbweb.nih.gov/ij/plugins/multitracker.html.
[11] A. A. Samarian and S. V. Vladimirov, "Charge of a macroscopic particle in a plasma sheath," *Phys. Rev. E*, vol. 67, no. 6, p. 066404, 2003.
[12] H. C. Lee, D. Y. Chen, and B. Rosenstein, "Phase diagram of crystals of dusty plasma," *Phys. Rev. E*, vol. 56, no. 4, p. 4596, 1997.
[13] H. Thomas, G. E. Morfill, V. Demmel, J. Goree, B. Feuerbacher, and D. Möhlmann, "Plasma crystal: Coulomb crystallization in a dusty plasma," *Phys. Rev. Lett.*, vol. 73, no. 5, p. 652, 1994.
[14] C. M. Ticoş, A. Dyson, and P. W. Smith, "The charge on falling dust particles in a RF plasma with DC negative bias," *Plasma Sources Sci. Technol.*, vol. 13, no. 3, p. 395, 2004.
[15] S. Kading, Y. Ivanov, and A. Melzer, "Stereoscopy on yukawa balls in dusty plasmas," *Plasma Sci. IEEE Trans. On*, vol. 35, no. 2, pp. 328–331, 2007.
[16] C. M. Ticos, D. Toader, M. L. Munteanu, N. Banu, and A. Scurtu, "High-speed imaging of dust particles in plasma," *J. Plasma Phys.*, vol. 79, no. 3, pp. 273–285, 2013.